Supplementary Materials

D.I. Larabi et al. - Insight does not come at random: Individual gray matter networks relate to clinical and cognitive insight in schizophrenia

Methods

Participants

Participants were enrolled in one of five clinical studies: (1) a study comparing the neural effects of aripiprazole and risperidone (EUDRA-CT: 2007-002748-79) (Liemburg *et al.* 2017), (2) a study examining the effect of repetitive transcranial magnetic stimulation on negative symptoms (trial number in Dutch trial register: NTR1261) (Dlabac-de Lange *et al.* 2015), (3) a study examining the neural basis of insight in affective and non-affective psychosis (Van der Meer *et al.* 2014), (4) a study examining a cognitive-emotional intervention aimed at improving insight (trial number in Dutch trial register: NTR1799) (Pijnenborg *et al.* 2011), and (5) a study examining the neural correlates of cognitive and emotion processing in healthy siblings of patients (van der Velde *et al.* 2014). Inclusion criteria for patients and healthy controls (HC) were age older than 18 years and being able to give informed consent. Exclusion criteria for patients were having an acute psychotic episode, having a comorbid neurological disorder, insufficient mastery of Dutch language, and MRI-contraindications. An exclusion criterion for HC was a lifetime axis I diagnosis. Additional inclusion criteria applied to two of these studies. Additional inclusion criteria, per study, were: a score of at least 15 on the negative subscale of the Positive and Negative Syndrome Scale interview (PANSS) (study 2) (Kay *et al.* 1987), impaired insight as defined by both rating by a clinician and a score lower than 10 on the Birchwood Insight Scale (BIS) (study 4) (Birchwood *et al.* 1994). Additional exclusion criteria applied to three of the studies. Additional exclusion criteria were, per study: rTMS contraindications (e.g. personal/family history of epilepsy, brain surgery or head injury with loss of consciousness in the past), previous treatment with rTMS, severe behavioral disorders and substance dependency within the previous 6 months (study 2), having a co-morbid psychiatric and/or somatic disorder, drug use, change of medication within the last week, use of a benzodiazepine equivalent to >3 mg lorazepam, electroconvulsive therapy within the last year (study

3), and receiving cognitive behavioral therapy (study 4). Additional inclusion criteria for HC of studies 4 and 5 were not having a history of somatic and/or neurological illnesses confirmed with the MINI-plus.

Data acquisition and preprocessing of structural MRI data

T1-weighted images were acquired in the Neuroimaging Center of the University Medical Center Groningen, the Netherlands, using a 3T MRI scanner equipped with an 8 channel SENSE head coil (Philips Intera, Best, Netherlands) (matrix size 256 mm x 256; FOV=256, 232, 170 mm; voxel size=1x0.9x1; TR=9 ms; TE=3.5 ms; 170 slices; duration=4 min 11 s). Scans were acquired parallel to the bicommissural plane, covering the whole brain.

Data was preprocessed using Statistical Parametric Mapping version 12 (SPM12; www.fil.ion.ucl.ac.uk/spm) implemented in Matlab R2015a (Mathworks Inc, Natick, MA). Preprocessing steps included manual reorientation to set the origin of the scans to the anterior commissure, and segmentation into gray matter (GM), white matter (WM), and cerebrospinal fluid (CSF) using unified segmentation. Quality of segmentations was checked for each GM segmentation individually, and by displaying one slice per individual and checking sample homogeneity using covariance in the VBM8 toolbox. This resulted in the exclusion of twelve patients and two healthy controls.

Construction of single-subject structural networks

A brain network was created per individual based on GM similarity. Consequently, each network was binarized by applying a subject-specific threshold of $p < 0.05$, which was determined with permutation testing. This resulted in unweighted and undirected networks. Subsequently, the following basic and higher-order graph metrics were computed for each individual using code of the Brain Connectivity Toolbox (BCT) (Rubinov & Sporns 2010): (1) size (i.e. number of nodes), (2) degree (i.e. number of edges) and (3) connectivity density (i.e. number of existing edges relative to the number of all

possible edges), (4) characteristic path length (L; i.e. the minimum number of edges between any two nodes), (5) clustering coefficient (CC; the fraction of node's neighbors that are each other's neighbors), and (6) betweenness centrality (BC; i.e. the proportion of paths that run through a specific node). In addition, per individual, 20 randomized reference networks with identical size, degree, and degree distribution were created and their higher-order graph metrics were calculated. Computation of graph metrics of individual and random networks was performed in Matlab 2018a on the high-performance computing facilities of the University of Groningen, the 'Peregrine' cluster multicore Dell comprised of 24 Intel Xeon 2.5 GHz cores. Subsequently, we calculated normalized path length (λ) and normalized clustering coefficient (γ) by dividing L and CC of each network, respectively, by those averaged from 20 random networks. Lastly, we computed small-world coefficients (σ) by dividing γ with λ. Networks show small-world topology when clustering coefficient is higher and path length is similar to that of random reference networks (i.e. when $\gamma/\lambda > 1$) (Watts & Strogatz 1998; Humphries & Gurney 2008). Graph metrics were computed on a global (i.e. averaged over the whole brain) as well as local level (i.e. averaged for 90 anatomical areas defined with the Automated Anatomical Labeling Atlas (AAL) atlas) (Tzourio-Mazoyer *et al.* 2002). To calculate local graph metrics per individual, an AAL-atlas was warped to subject space with inverse normalization parameters obtained during segmentation. Per individual, subject space GM segmentations were then parcellated into 90 areas with the AAL-atlas. Nodes were labeled according to the most frequently occurring AAL-label of a node's voxels. Graph metrics per node were averaged within an AAL-area to obtain local graph metrics per AAL-area. The AAL-parcellation was chosen to be consistent with previous studies using the same methodology so that results could be compared to existing literature.

Results

Testing the effect of standardized antipsychotic dose on the relationship between graph metrics and insight

We checked the influence of standardized antipsychotic dose on GM networks by repeating analyses including standardized antipsychotic dose as an additional covariate. Effect sizes remained highly similar when controlling for standardized antipsychotic dose. Specifically, for clinical insight, in the sample of 62 patients, the correlation between PANSS G12 and betweenness centrality remained highly similar (from r_s=0.31, p=0.01 to r_s=0.31, p=0.02), just as the correlation between SAI-E Relabeling of symptoms and clustering coefficient (from r_s=0.30, p=0.02 to r_s=0.29, p=0.03). For cognitive insight, the correlations also remained highly similar: BCIS composite index and normalized path length (from r_s=0.27, p=0.04 to r_s=0.27, p=0.04), normalized clustering coefficient (from r_s=0.30, p=0.02 to r_s=0.29, p=0.03) and small-world coefficient (from r_s=0.31, p=0.01 to r_s=0.30, p=0.02); BCIS self-certainty and normalized clustering coefficient (from r_s=-0.31, p=0.02 to r_s=-0.29, p=0.02) and small-world coefficients (r_s=-0.33, p=0.01 to r_s=-0.31, p=0.02). Correlations between local graph metrics and insight also remained similar with additional correction for standardized antipsychotic dose.

Testing the effect of age and sex

Group comparisons of global graph metrics controlling for age and sex.

Results of group comparisons controlling for age and sex were similar (Supplementary Table S5). After regressing out sex and age, we still found lower segregation (i.e. clustering coefficient) and higher centrality (i.e. betweenness centrality) of the gray matter connectomes of 114 patients compared to HC. Results were also unchanged when including only schizophrenia patients (n=97 sample). The only change in results after correction for sex and age is that the difference in betweenness centrality

between 62 patients and HC became insignificant after FDR-correction (but significant without FDR-correction).

Group comparisons of local graph metrics controlling for age and sex.

Locally, after additional correction for age and sex, similarly to results without this additional correction, we found significantly lower normalized path length and clustering coefficient in several areas in patients compared to HC (Table S6 and Figure S5). The differences in normalized clustering coefficient and small-world coefficients of the right calcarine sulcus were not significant anymore in the full sample, but, in contrast, in the smaller subsample only including patients diagnosed with schizophrenia (n=97).

Correlations between global graph metrics and insight controlling for age and sex

Clinical insight in 114 patients.

The correlations between global graph metrics and PANSS G12 scores were highly similar after regressing out age and sex. However, the significant positive correlation between higher PANSS G12 scores and higher betweenness centrality in the n=62 sample was not significant anymore after FDR-correction but only significant at trend-level (Table S7).

Clinical and cognitive insight in 62 patients.

The correlations between global graph metrics and SAI-E scores were also similar after regressing out age and sex. The significant correlation between SAI-E Relabeling of symptoms and clustering coefficient became significant at trend-level. Furthermore, additional correlations significant at trend-level were seen between SAI-E Relabeling of symptoms and betweenness centrality, and between SAI-E Awareness of illness and normalized path length.

With regard to cognitive insight, the significant correlations between BCIS composite index scores and normalized path length, normalized clustering coefficient and small-world coefficients became significant at trend-level. The significant correlation between BCIS composite index scores and path length was not significant anymore. For the self-certainty subscale of the BCIS, the significant correlation with small-world coefficient became significant at trend-level. The significant correlation with normalized clustering coefficient was not significant anymore (Table S8).

Correlations between local graph metrics and insight controlling for age and sex.

With regard to PANSS G12 scores, the three significant correlations with path length were not significant anymore. Of the two significant correlations with betweenness centrality, one remained significant. The significant correlation with normalized path length of the left anterior cingulate gyrus remained significant.

For SAI-E Awareness of illness scores the significant correlations with path length of two areas remained significant, while one area was added. The significant correlations with normalized path length of two areas remained significant, in addition to two additional areas. For SAI-E Relabeling of symptoms, the significant correlations with clustering coefficient of four areas remained significant, in addition to four extra areas. Furthermore, an additional significant correlation with normalized path length of the left anterior cingulate gyrus was seen.

With regard to cognitive insight, seven out of sixteen significant correlations between BCIS composite index scores and path length remained significant. Significant correlations between BCIS composite index scores and betweenness centrality were not significant anymore. Four out of nine significant correlations with normalized path length remained significant. One of nine significant correlations with normalized clustering coefficient remained significant, and three out of five significant correlations with small-world coefficients. For BCIS self-reflectiveness, the number of significant

correlations with path length, normalized path length, normalized clustering coefficient and small-world coefficients reduced (from five to four, seven to four, and five to three, respectively) while the number of significant correlations with normalized path length increased (from three to four). The significant correlations between BCIS self-certainty and path length, normalized clustering coefficient and small-world coefficient were not significant anymore (Table S9).

Tables

Table S1. Means of insight measures and intercorrelations between insight measures.

Insight	Mean (SD)	G12	SAIE AI	SAIE RS	SAIE NT	SAIE sub
G12	3.04 (1.57)		**r_s=-0.61, p<0.001****	**r_s=-0.62, p<0.001****	**r_s=-0.47, p<0.001****	**r_s=-0.69, p<0.001****
BCIS SR	13.87 (4.79)	r_s=-0.23, p= 0.07	r_s=0.12, p=0.37	r_s=0.16, p=0.23	r_s=0.05, p=0.69	r_s=0.11, p=0.38
BCIS SC	8.24 (3.26)	r_s=0.20, p= 0.12	**r_s=-0.25, p=0.047***	r_s=-0.14, p= 0.29	**r_s=-0.30, p=0.018***	r_s=-0.23, p=0.07
BCIS ci	5.63 (5.44)	**r_s=-0.33, p=0.008***	r_s=0.24, p= 0.06	r_s=0.17, p=0.19	r_s=0.23, p=0.08	r_s=0.22, p=0.08
SAIE AI	8.02 (3.18)					
SAIE RS	3.08 (1.94)					
SAIE NT	1.47 (0.72)					
SAIE sub	14.51 (5.74)					

PANSS G12 data were available for 114 patients; SAI-E and BCIS data were available for a subsample of 62 patients. Better insight is reflected by lower PANSS G12 scores, higher SAI-E scores, higher BCIS self-reflectiveness (SR), and composite index (ci) scores and lower BCIS self-certainty (SC) scores.
*Significant p<0.05.
**Significant p<0.001.
Abbreviations: G12=item 12 of the General Psychopathology subscale of the Positive and Negative Syndrome Scale; SAIE=Schedule for Assessment of Insight – Expanded; AI=Awareness of illness; RS=Relabeling of symptoms; NT=Need for treatment; sub=subtotal score; BCIS=Beck Cognitive Insight Scale; SR=self-reflectiveness; SC=self-certainty; ci=composite index score.

Table S2. Spearman correlations between insight measures and participant-, gray matter network-, and illness characteristics.

Insight	G12	SAIE AI	SAIE RS	SAIE NT	SAIE sub	BCIS SR	BCIS SC	BCIS ci
Gray matter network characteristics								
Size	0.03	-0.13	-0.17	-0.14	-0.12	0.01	0.25	-0.09
Degree	-0.01	-0.10	0.02	-0.12	-0.08	-0.004	0.25	-0.12
Density	-0.05	0.07	0.27	-0.01	0.04	-0.03	0.06	-0.07
Total GMV	-0.10	0.02	0.06	-0.13	0.03	0.24	0.16	0.14
Total WMV	0.09	-0.19	-0.22	-0.10	-0.19	-0.24	0.26	-0.32
Total CSF	0.08	-0.16	-0.16	-0.18	-0.10	0.03	0.16	-0.07
Participant characteristics								
Age	0.15	-0.02	-0.05	0.02	-0.04	-0.22	0.16	-0.27
Education	-0.19	0.26	-0.004	0.08	0.16	0.09	-0.10	0.10
Sex[a]	0.72	0.01	0.002	0.14	0.16	1.44	3.12	0.0001
Handedness[a]	0.75	0.003	0.12	1.90	0.22	0.23	0.91	1.00
Illness characteristics								
Illness duration	0.14	0.06	0.04	0.04	0.09	-0.18	0.26	-0.27
Standardized antipsychotic dose	0.09	-0.02	-0.05	0.01	0.01	-0.07	0.32	-0.20
PANSS positive symptoms	0.31	-0.28	**-0.47***	-0.34	-0.37	0.09	0.09	0.03
PANSS negative symptoms	0.14	-0.06	-0.09	-0.10	-0.11	-0.07	0.17	-0.15
PANSS global symptoms minus G12	0.12	-0.04	-0.17	-0.16	-0.12	0.02	0.08	-0.05

[a] Differences in insight for sex and handedness were tested with ANOVA's, reported are F-statistics (between-groups degrees of freedom: 1; within-groups degrees of freedom: 113).
*Significant at $p<0.05$ after FDR-correction for 120 tests (i.e. 15 participant-, gray matter network-, and illness characteristics * 8 insight measures).
Abbreviations: G12=item 12 of the General Psychopathology subscale of the Positive and Negative Syndrome Scale; SAIE=Schedule for Assessment of Insight – Expanded; AI=Awareness of illness; RS=Relabeling of symptoms; NT=Need for treatment; sub=subtotal score; BCIS=Beck Cognitive Insight Scale; SR=self-reflectiveness; SC=self-certainty; ci=composite index score; GMV=gray matter volume; WMV=white matter volume; CSF=cerebrospinal fluid; PANSS=Positive and Negative Syndrome Scale.

Table S3. Comparison of global gray matter network measures between patients and healthy controls.

Network measure	Difference between groups[a]	Difference between groups[b]
Path length (L)	F(1,148)=0.0005, p=0.98	F(1,114)=0.02, p=0.89
Clustering coefficient (CC)	**F(1,148)=19.02, p_{FDR}<0.001****	**F(1,114)= 14.82, p_{FDR}=0.001***
Betweenness centrality (BC)	**F(1,148)=9.14, p=0.003, p_{FDR}=0.009***	F(1,114)= 5.46, p=0.02, p_{FDR}=.06
Normalized path length (λ)	F(1,148)=3.46, p=.07, p_{FDR}=0.08	F(1,114)= 2.84, p=0.10
Normalized clustering coefficient (γ)	F(1,148)=4.35, p=0.04, p_{FDR}=0.06	F(1,114)=3.51, p=0.06
Small-world coefficient (σ)	F(1,148)=4.58, p=0.03, p_{FDR}=0.06	F(1,114)=3.60, p=0.06

Corrected for education and total gray matter volume.

[a]n=97 patients, only including patients with schizophrenia, and 54 HC.

[b]n=62 patients, and 54 HC.

*Significant p<0.05.

**Significant p<0.001.

Table S4. Comparison of local gray matter network measures between patients and healthy controls.

Network measure/AAL-area	Mean (SD) patients (n=114)	Mean (SD) healthy controls (n=54)	Difference between groups[a]	Difference between groups[b]	Difference between groups[c]
Differences in path length					
47. Left lingual gyrus	In n=151 sample: 2.11 (0.06)	2.08 (0.06)	n.s.	F(1,143)=9.28, p_{FDR}=0.03	n.s.
48. Right lingual gyrus	In n=151 sample: 2.1 (0.05)	2.08 (0.06)	n.s.	F(1,143)=7.65, p_{FDR}=0.04	n.s.
Differences in clustering coefficient					
1. Left precentral gyrus	0.42 (0.03)	0.44 (0.03)	F(1,160)=16.54, p_{FDR}=0.01	similar	similar
2. Right precentral gyrus	0.43 (0.03)	0.44 (0.03)	F(1,160)=14.01, p_{FDR}=0.01	similar	similar
3. Left superior frontal gyrus	0.45 (0.02)	0.46 (0.02)	F(1,160)=22.52, p_{FDR}=0.002	similar	similar
4. Right superior frontal gyrus	0.45 (0.02)	0.46 (0.03)	F(1,160)=11.53, p_{FDR}=0.02	similar	similar
7. Left middle frontal gyrus	In n=151 sample: 0.42 (0.03)	0.44 (0.03)	n.s.	F(1,138)=8.52, p_{FDR}=0.03	n.s.
8. Right middle frontal gyrus	0.42 (0.03)	0.44 (0.03)	F(1,159)=17.20, p_{FDR}=0.01	similar	similar
11. Left inferior frontal opercularis	In n=151 sample: 0.43 (0.03)	0.44 (0.03)	n.s.	F(1,131)=7.27, p_{FDR}=0.047	n.s.
12. Right inferior frontal opercularis	In n=151 sample: 0.43 (0.03)	0.45 (0.03)	n.s.	F(1,127)=9.61, p_{FDR}=0.03	n.s.
13. Left inferior frontal triangularis	0.42 (0.03)	0.44 (0.03)	F(1,154)=9.33, p_{FDR}=0.04	similar	similar
14. Right inferior frontal triangularis	0.43 (0.03)	0.45 (0.03)	F(1,159)=19.24, p_{FDR}=0.003	similar	similar
18. Right Rolandic operculum	In n=151 sample: 0.38 (0.05)	0.42 (0.07)	n.s.	F(1,143)=9.18, p_{FDR}=0.03	n.s.
20. Right supplementary motor area	0.41 (0.04)	0.43 (0.03)	F(1,160)=11.72, p_{FDR}=0.02	similar	similar
27. Left rectal gyrus	0.42 (0.06)	0.47 (0.06)	F(1,157)=13.31, p_{FDR}=0.01	similar	similar
28. Right rectal gyrus	0.42 (0.05)	0.45 (0.06)	F(1,156)=10.14, p_{FDR}=0.03	similar	n.s.
29. Left insula	In n=151 sample: 0.42 (0.06)	0.46 (0.08)	n.s.	F(1,143)=7.80, p_{FDR}=0.04	n.s.

Network measure/AAL-area	Mean (SD) patients (n=114)	Mean (SD) healthy controls (n=54)	Difference between groups[a]	Difference between groups[b]	Difference between groups[c]
35. Left posterior cingulate gyrus	0.47 (0.05)	0.49 (0.05)	F(1,160)=12.27, p_{FDR}=0.01	similar	similar
37. Left hippocampus	In n=151 sample: 0.42 (0.04)	0.44 (0.05)	n.s.	F(1,143)=7.20, p_{FDR}=0.047	n.s.
38. Right hippocampus	0.43 (0.04)	0.45 (0.04)	F(1,160)=9.09, p_{FDR}=0.04	similar	n.s.
41. Left amygdala	In n=151 sample: 0.40 (0.04)	0.42 (0.05)	n.s.	F(1,143)=7.21, p_{FDR}=0.047	n.s.
42. Right amygdala	In n=151 sample: 0.41 (0.03)	0.43 (0.04)	n.s.	F(1,143)=9.05, p_{FDR}=0.03	n.s.
43. Left calcarine sulcus	0.39 (0.04)	0.41 (0.04)	F(1,160)=9.36, p_{FDR}=0.04	similar	n.s.
44. Right calcarine sulcus	0.39 (0.04)	0.41 (0.04)	F(1,160)=15.48, p_{FDR}=0.01	similar	similar
45. Left cuneus	0.36 (0.03)	0.38 (0.03)	F(1,160)=14.34, p_{FDR}=0.01	similar	similar
46. Right cuneus	0.38 (0.04)	0.4 (0.05)	F(1,160)=9.16, p_{FDR}=0.04	similar	n.s.
50. Right superior occipital gyrus			n.s.	F(1,143)=7.77, p_{FDR}=0.04	n.s.
51. Left middle occipital gyrus	0.42 (0.03)	0.43 (0.04)	F(1,160)=15.73, p_{FDR}=0.01	similar	similar
52. Right middle occipital gyrus	0.42 (0.03)	0.44 (0.04)	F(1,160)=16.56, p_{FDR}=0.01	similar	similar
56. Right fusiform gyrus	0.41 (0.03)	0.42 (0.03)	F(1,160)=8.83, p_{FDR}=0.05	similar	n.s.
57. Left postcentral gyrus	0.40 (0.03)	0.42 (0.03)	F(1,160)=18.41, p_{FDR}=0.003	similar	similar
58. Right postcentral gyrus	0.41 (0.03)	0.43 (0.02)	F(1,160)=14.12, p_{FDR}=0.01	similar	similar
59. Left superior parietal gyrus	In n=151 sample: 0.39 (0.03)	0.40 (0.03)	n.s.	F(1,143)=9.23, p_{FDR}=0.03	n.s.
60. Right superior parietal gyrus	0.39 (0.04)	0.40 (0.04)	F(1,160)=11.84, p_{FDR}=0.02	similar	similar
61. Left inferior parietal gyrus	0.41 (0.03)	0.42 (0.03)	F(1,160)=12.69, p_{FDR}=0.01	similar	similar
63. Left supramarginal gyrus	0.40 (0.03)	0.41 (0.03)	F(1,160)=12.49, p_{FDR}=0.01	similar	similar
64. Right supramarginal gyrus	0.40 (0.03)	0.42 (0.03)	F(1,160)=11.79, p_{FDR}=0.02	similar	similar
65. Left angular gyrus	0.41 (0.03)	0.42 (0.03)	F(1,160)=13.40, p_{FDR}=0.01	similar	similar
66. Right angular gyrus	In n=151 sample: 0.41 (0.03)	0.42 (0.03)	n.s.	F(1,143)=9.10, p_{FDR}=0.03	n.s.

Network measure/AAL-area	Mean (SD) patients (n=114)	Mean (SD) healthy controls (n=54)	Difference between groups[a]	Difference between groups[b]	Difference between groups[c]
67. Left precuneus	0.37 (0.03)	0.39 (0.03)	$F(1,160)=12.67$, $p_{FDR}=0.01$	similar	similar
70. Right paracentral lobule	0.39 (0.04)	0.41 (0.04)	$F(1,160)=9.53$, $p_{FDR}=0.04$	similar	similar
73. Left putamen	0.43 (0.03)	0.45 (0.03)	$F(1,160)=20.86$, $p_{FDR}=0.002$	similar	similar
74. Right putamen	0.45 (0.03)	0.44 (0.03)	$F(1,160)=12.64$, $p_{FDR}=0.01$	similar	similar
75. Left pallidum	0.47 (0.06)	0.47 (0.06)	$F(1,160)=12.05$, $p_{FDR}=0.01$	similar	similar
80. Right Heschl's gyrus	0.46 (0.07)	0.48 (0.06)	$F(1,160)=13.23$, $p_{FDR}=0.01$	similar	similar
81. Left superior temporal gyrus	0.42 (0.04)	0.45 (0.03)	$F(1,160)=14.25$, $p_{FDR}=0.01$	similar	n.s.
82. Right superior temporal gyrus	0.42 (0.04)	0.45 (0.03)	$F(1,160)=12.59$, $p_{FDR}=0.01$	similar	similar
84. Right temporal pole	In n=151 sample: 0.44 (0.03)	0.44 (0.03)	n.s.	$F(1,143)=10.98$, $p_{FDR}=0.02$	$F(1,109)=10.16$, $p_{FDR}=0.03$
85. Left middle temporal gyrus	0.42 (0.03)	0.44 (0.03)	$F(1,160)=21.97$, $p_{FDR}=0.002$	similar	similar
86. Right middle temporal gyrus	In n=151 sample: 0.42 (0.03)	0.45 (0.03)	n.s.	$F(1,142)=7.23$, $p_{FDR}=0.047$	n.s.
89. Left inferior temporal gyrus	In n=151 sample: 0.44 (0.04)	0.46 (0.05)	n.s.	$F(1,143)=8.64$, $p_{FDR}=0.03$	n.s.
Difference in betweenness centrality					
2. Right precentral gyrus	In n=151 sample: 7130.65 (1096.72)	6659.30 (995.60)	n.s.	$F(1,143)=7.74$, $p_{FDR}=0.04$	n.s.
68. Right precuneus	In n=151 sample: 6932.93 (1035.10)	6706.31 (1166.47)	n.s.	$F(1,142)=7.07$, $p_{FDR}=0.046$	n.s.
Difference in normalized path length (λ)					
2. Right precentral gyrus	In n=151 sample: 1.04 (0.02)	1.05 (0.02)	n.s.	$F(1,143)=8.67$, $p_{FDR}=0.03$	n.s.
8. Right middle frontal gyrus	In n=151 sample: 1.05 (0.01)	1.06 (0.01)	n.s.	$F(1,142)=7.21$, $p_{FDR}=0.047$	n.s.
13. Left inferior frontal triangularis	In n=151 sample: 1.05 (0.02)	1.07 (0.02)	n.s.	$F(1,137)=8.45$, $p_{FDR}=0.03$	n.s.
14. Right inferior frontal triangularis	1.06 (0.02)	1.07 (0.02)	$F(1,159)=9.91$, $p_{FDR}=0.03$	similar	n.s.

Network measure/AAL-area	Mean (SD) patients (n=114)	Mean (SD) healthy controls (n=54)	Difference between groups[a]	Difference between groups[b]	Difference between groups[c]
26. Right superior frontal gyrus, medial orbital	In n=151 sample: 1.07 (0.02)	1.08 (0.02)	n.s.	F(1,142)=8.66, p_{FDR}=0.03	F(1,108)=9.29, p_{FDR}=0.04
46. Right cuneus	1.04 (0.02)	1.06 (0.03)	F(1,160)=12.11, p_{FDR}=0.01	similar	similar
57. Left postcentral gyrus	In n=151 sample: 1.05 (0.02)	1.06 (0.03)	n.s.	F(1,143)=8.41, p_{FDR}=0.03	n.s.
58. Right postcentral gyrus	In n=151 sample: 1.04 (0.02)	1.06 (0.03)	n.s.	F(1,142)=9.49, p_{FDR}=0.03	
69. Left paracentral lobule	1.03 (0.02)	1.05 (0.02)	F(1,160)=9.81, p_{FDR}=0.03	similar	similar
77. Left thalamus	In n=151 sample: 1.07 (0.02)	1.08 (0.02)	n.s.	F(1,143)=8.95, p_{FDR}=0.03	
81. Left superior temporal gyrus	In n=151 sample: 1.07 (0.01)	1.07 (0.02)	n.s.	F(1,143)=9.44, p_{FDR}=0.03	n.s.
Difference in normalized clustering coefficient (γ)					
1. Left precentral gyrus	In n=151 sample: 1.55 (0.14)	1.63 (0.1)	n.s.	F(1,143)=9.03, p_{FDR}=0.03	F(1,109)=11.43, p_{FDR}=0.02
2. Right precentral gyrus	In n=151 sample: 1.56 (0.13)	1.64 (0.11)	n.s.	F(1,143)=10.14, p_{FDR}=0.02	F(1,109)=10.11, p_{FDR}=0.03
3. Left superior frontal gyrus, dorsolateral	In n=151 sample: 1.65 (0.13)	1.73 (0.12)	n.s.	F(1,143)=7.29, p_{FDR}=0.047	n.s.
8. Right middle frontal gyrus	In n=151 sample: 1.54 (0.14)	1.62 (0.11)	n.s.	F(1,142)=8.16, p_{FDR}=0.04	n.s.
14. Right inferior frontal gyrus triangularis	In n=151 sample: 1.58 (0.15)	1.66 (0.11)	n.s.	F(1,142)=10.19, p_{FDR}=0.02	n.s.
27. Left gyrus rectus	In n=151 sample: 1.55 (0.28)	1.74 (0.28)	n.s.	F(1,140)=7.96, p_{FDR}=0.04	F(1,106)=13.26, p_{FDR}=0.01
35. Left posterior cingulate gyrus	In n=151 sample: 1.72 (0.23)	1.83 (0.19)	n.s.	F(1,143)=8.35, p_{FDR}=0.03	n.s.
44. Right calcarine sulcus	1.42 (0.19)	1.52 (0.16)	F(1,160)=9.16, p_{FDR}=0.04	similar	n.s.
45. Left cuneus	In n=151 sample: 1.32 (0.14)	1.40 (0.13)	n.s.	F(1,143)=8.58, p_{FDR}=0.03	n.s.

Network measure/AAL-area	Mean (SD) patients (n=114)	Mean (SD) healthy controls (n=54)	Difference between groups[a]	Difference between groups[b]	Difference between groups[c]
51. Left middle occipital gyrus	In n=151 sample: 1.53 (0.16)	1.59 (0.14)	n.s.	F(1,143)=8.33, p_{FDR}=0.03	n.s.
52. Right middle occipital gyrus	In n=151 sample: 1.53 (0.15)	1.61 (0.14)	n.s.	F(1,143)=9.93, p_{FDR}=0.02	n.s.
57. Left postcentral gyrus	In n=151 sample: 1.47 (0.14)	1.55 (0.12)	n.s.	F(1,143)=10.18, p_{FDR}=0.02	F(1,109)=11.89, p_{FDR}=0.02
58. Right postcentral gyrus	In n=151 sample: 1.50 (0.14)	1.56 (0.11)	n.s.	F(1,143)=7.53, p_{FDR}=0.04	n.s.
67. Left precuneus	In n=151 sample: 1.35 (0.15)	1.43 (0.1)	n.s.	F(1,143)=7.38, p_{FDR}=0.04	n.s.
73. Left putamen	In n=151 sample: 1.59 (0.15)	1.66 (0.15)	n.s.	F(1,143)=8.06, p_{FDR}=0.04	n.s.
80. Right Heschl gyrus	In n=151 sample: 1.69 (0.29)	1.79 (0.24)	n.s.	F(1,143)=9.63, p_{FDR}=0.03	n.s.
85. Left middle temporal gyrus	In n=151 sample: 1.56 (0.15)	1.65 (0.13)	n.s.	F(1,143)=10.56, p_{FDR}=0.02	F(1,109)=11.79, p_{FDR}=0.02
Difference in small-world coefficient (σ)					
1. Left precentral gyrus	In n=151 sample: 1.49 (0.11)	1.55 (0.09)	n.s.	F(1,143)=8.81, p_{FDR}=0.03	F(1,109)=11.26, p_{FDR}=0.02
2. Right precentral gyrus	In n=151 sample: 1.50 (0.11)	1.56 (0.09)	n.s.	F(1,143)=9.46, p_{FDR}=0.03	F(1,109)=9.66, p_{FDR}=0.03
3. Left superior frontal gyrus, dorsolateral	In n=151 sample: 1.57 (0.11)	1.63 (0.10)	n.s.	F(1,141)=7.61, p_{FDR}=0.04	n.s.
8. Right middle frontal gyrus	In n=151 sample: 1.46 (0.12)	1.52 (0.09)	n.s.	F(1,142)=7.93, p_{FDR}=0.04	n.s.
14. Right inferior frontal gyrus triangularis	In n=151 sample: 1.49 (0.13)	1.55 (0.10)	n.s.	F(1,142)=8.62, p_{FDR}=0.03	n.s.
27. Left gyrus rectus	In n=151 sample: 1.44 (0.25)	1.60 (0.23)	n.s.	F(1,140)=8.09, p_{FDR}=0.04	F(1,106)=14.38, p_{FDR}=0.01
35. Left posterior cingulate gyrus	In n=151 sample: 1.62 (0.21)	1.71 (0.17)	n.s.	F(1,141)=7.45, p_{FDR}=0.04	n.s.
44. Right calcarine sulcus	1.33 (0.18)	1.42 (0.15)	F(1,160)=9.30, p_{FDR}=0.04	similar	n.s.

Network measure/AAL-area	Mean (SD) patients (n=114)	Mean (SD) healthy controls (n=54)	Difference between groups[a]	Difference between groups[b]	Difference between groups[c]
45. Left cuneus	In n=151 sample: 1.25 (0.12)	1.32 (0.11)	n.s.	F(1,143)=7.89, p_{FDR}=0.04	n.s.
51. Left middle occipital gyrus	In n=151 sample: 1.44 (0.14)	1.48 (0.13)	n.s.	F(1,143)=8.83, p_{FDR}=0.03	n.s.
52. Right middle occipital gyrus	In n=151 sample: 1.44 (0.14)	1.51 (0.13)	n.s.	F(1,143)=10.09, p_{FDR}=0.02	n.s.
57. Left postcentral gyrus	In n=151 sample: 1.41 (0.13)	1.46 (0.11)	n.s.	F(1,143)=7.82, p_{FDR}=0.04	F(1,109)=9.17, p_{FDR}=0.04
73. Left putamen	In n=151 sample: 1.48 (0.13)	1.53 (0.13)	n.s.	F(1,143)=7.75, p_{FDR}=0.04	n.s.
80. Right Heschl gyrus	In n=151 sample: 1.60 (0.27)	1.68 (0.23)	n.s.	F(1,143)=8.10, p_{FDR}=0.04	n.s.
85. Left middle temporal gyrus	In n=151 sample: 1.45 (0.13)	1.53 (0.11)	n.s.	F(1,143)=10.54, p_{FDR}=0.02	F(1,109)=11.81, p_{FDR}=0.02

Corrected for education, total and local gray matter volume. Only differences significant after FDR-correction for 540 tests are shown.

[a]Including 114 patients and 54 healthy controls (total n=168).

[b]Only including patients with schizophrenia (n=97) and healthy controls (n=54) (total n=151).

[c]Only including patients for whom additional insight measures were available (n=62) and healthy controls (n=54) (total n=116).

Abbreviations: SD=standard deviation; AAL=automated anatomical labeling; n.s.=not significant; similar=similar as in whole sample.

Table S5. Comparison of global gray matter network measures between patients and healthy controls with additional correction for age and sex.

Network measure	Difference between groups[a]	Difference between groups[b]	Difference between groups[c]
Path length (L)	F(1,163)=0.13, p=0.71	F(1,146)=0.12, p=0.73	F(1,112)=0.67, p=0.42
Clustering coefficient (CC)	**F(1,163)=16.45, p<0.001, p_{FDR}<0.001****	**F(1,146)=17.31, p<0.001, p_{FDR}<0.001****	**F(1,112)= 12.63, p<0.001, p_{FDR}=0.003***
Betweenness centrality (BC)	**F(1,163)=9.38, p=0.003, p_{FDR}=0.01***	**F(1,146)=10.34, p=0.002, p_{FDR}=0.004***	F(1,112)= 4.28, p=0.04, p_{FDR}=0.12
Normalized path length (λ)	F(1,163)=2.07, p=.15	F(1,146)=2.27, p=0.13, p_{FDR}=0.08	F(1,112)= 1.09, p=0.30
Normalized clustering coefficient (γ)	F(1,163)=2.42, p=.12	F(1,146)=3.22, p=0.08, p_{FDR}=0.06	F(1,112)=1.65, p=0.20
Small-world coefficient (σ)	F(1,163)=2.53, p=0.11	F(1,146)=3.47, p=0.07, p_{FDR}=0.06	F(1,112)=1.74, p=0.19

Corrected for education, total gray matter volume, age and sex. FDR-correction for 6 tests.

[a]114 patients with a psychotic disorder and 54 HC.

[b]n=97 patients, only including patients with schizophrenia, and 54 HC.

[c]n=62 patients, only including patients with schizophrenia for whom detailed insight measures were available, and 54 HC.

*Significant p_{FDR}<0.05.

*Significant p_{FDR}<0.001.

Table S6. Comparison of local gray matter network measures between patients and healthy controls with additional correction for age and sex.

Network measure/AAL-area	Mean (SD) patients (n=114)	Mean (SD) healthy controls (n=54)	Difference between groups[a]	Difference between groups[b]	Difference between groups[c]
Differences in path length					
47. Left lingual gyrus	In n=151 sample: 2.11 (0.06)	2.08 (0.06)	n.s.	F(1,143)=8.83, p_{FDR}=0.04	n.s.
48. Right lingual gyrus	In n=151 sample: 2.10 (0.05)	2.08 (0.06)	n.s.	F(1,143)=7.60, p_{FDR}=0.045	n.s.
Differences in clustering coefficient					
1. Left precentral gyrus	0.42 (0.03)	0.44 (0.03)	F(1,160)=16.09, p_{FDR}=0.01	similar	similar
2. Right precentral gyrus	0.43 (0.03)	0.44 (0.03)	F(1,160)=13.56, p_{FDR}=0.01	similar	similar
3. Left superior frontal gyrus	0.45 (0.02)	0.46 (0.02)	F(1,160)=22.85, p_{FDR}=0.001	similar	similar
4. Right superior frontal gyrus	0.45 (0.02)	0.46 (0.03)	F(1,160)=11.26, p_{FDR}=0.02	similar	similar
7. Left middle frontal gyrus	In n=151 sample: 0.42 (0.03)	0.44 (0.03)	n.s.	F(1,138)=7.51, p_{FDR}=0.046	n.s.
8. Right middle frontal gyrus	0.42 (0.03)	0.44 (0.03)	F(1,159)=17.13, p_{FDR}=0.01	similar	similar
11. Left inferior frontal opercularis	0.43 (0.03)	0.44 (0.03)	F(1,147)=9.30, p_{FDR}=0.04	similar	n.s.
12. Right inferior frontal opercularis	In n=151 sample: 0.43 (0.03)	0.45 (0.03)	n.s.	F(1,127)=10.67, p_{FDR}=0.02	n.s.
13. Left inferior frontal triangularis	0.42 (0.03)	0.44 (0.03)	F(1,154)=10.40, p_{FDR}=0.03	similar	similar
14. Right inferior frontal triangularis	0.43 (0.03)	0.45 (0.03)	F(1,159)=20.04, p_{FDR}=0.002	similar	similar
18. Right Rolandic operculum	In n=151 sample: 0.38 (0.05)	0.42 (0.07)	n.s.	F(1,143)=9.74, p_{FDR}=0.03	n.s.
20. Right supplementary motor area	0.41 (0.04)	0.43 (0.03)	F(1,160)=11.19, p_{FDR}=0.02	similar	similar
27. Left rectal gyrus	0.42 (0.06)	0.47 (0.06)	F(1,157)=13.05, p_{FDR}=0.01	similar	similar
28. Right rectal gyrus	0.42 (0.05)	0.45 (0.06)	F(1,156)=9.75, p_{FDR}=0.03	similar	n.s.
35. Left posterior cingulate gyrus	0.47 (0.05)	0.49 (0.05)	F(1,160)=12.02, p_{FDR}=0.02	similar	similar

Network measure/AAL-area	Mean (SD) patients (n=114)	Mean (SD) healthy controls (n=54)	Difference between groups[a]	Difference between groups[b]	Difference between groups[c]
38. Right hippocampus	In n=151 sample: 0.43 (0.04)	0.45 (0.04)	n.s.	F(1,143)=8.21, p_{FDR}=0.04	n.s.
42. Right amygdala	In n=151 sample: 0.41 (0.03)	0.43 (0.04)	n.s.	F(1,143)=8.70, p_{FDR}=0.04	n.s.
43. Left calcarine sulcus	0.39 (0.04)	0.41 (0.04)	F(1,160)=8.93, p_{FDR}=0.047	similar	n.s.
44. Right calcarine sulcus	0.39 (0.04)	0.41 (0.04)	F(1,160)=14.64, p_{FDR}=0.01	similar	similar
45. Left cuneus	0.36 (0.03)	0.38 (0.03)	F(1,160)=14.05, p_{FDR}=0.01	similar	similar
46. Right cuneus	0.38 (0.04)	0.40 (0.05)	F(1,160)=8.91, p_{FDR}=0.047	similar	n.s.
51. Left middle occipital gyrus	0.42 (0.03)	0.43 (0.04)	F(1,160)=15.31, p_{FDR}=0.01	similar	similar
52. Right middle occipital gyrus	0.42 (0.03)	0.44 (0.04)	F(1,160)=16.05, p_{FDR}=0.01	similar	similar
56. Right fusiform gyrus	In n=151 sample: 0.40 (0.03)	0.41 (0.03)	n.s.	F(1,143)=10.81, p_{FDR}=0.02	n.s.
57. Left postcentral gyrus	0.40 (0.03)	0.42 (0.03)	F(1,160)=18.26, p_{FDR}=0.004	similar	similar
58. Right postcentral gyrus	0.41 (0.03)	0.43 (0.02)	F(1,160)=13.25, p_{FDR}=0.01	similar	similar
59. Left superior parietal gyrus	In n=151 sample: 0.39 (0.03)	0.40 (0.03)	n.s.	F(1,143)=8.43, p_{FDR}=0.04	n.s.
60. Right superior parietal gyrus	0.39 (0.04)	0.40 (0.04)	F(1,160)=11.05, p_{FDR}=0.02	similar	n.s.
61. Left inferior parietal lobule	0.41 (0.03)	0.42 (0.03)	F(1,160)=12.33, p_{FDR}=0.01	similar	similar
63. Left supramarginal gyrus	0.40 (0.03)	0.41 (0.03)	F(1,160)=13.25, p_{FDR}=0.01	similar	similar
64. Right supramarginal gyrus	0.40 (0.03)	0.42 (0.03)	F(1,160)=11.81, p_{FDR}=0.02	similar	similar
65. Left angular gyrus	0.41 (0.03)	0.42 (0.03)	F(1,160)=13.59, p_{FDR}=0.01	similar	similar
66. Right angular gyrus	In n=151 sample: 0.41 (0.03)	0.42 (0.03)	n.s.	F(1,143)=8.42, p_{FDR}=0.04	n.s.
67. Left precuneus	0.37 (0.03)	0.39 (0.03)	F(1,160)=12.04, p_{FDR}=0.02	similar	similar
70. Right paracentral lobule	0.39 (0.04)	0.41 (0.04)	F(1,160)=9.02, p_{FDR}=0.047	similar	similar
73. Left putamen	0.43 (0.03)	0.45 (0.03)	F(1,160)=20.84, p_{FDR}=0.002	similar	similar
74. Right putamen	0.44 (0.03)	0.45 (0.03)	F(1,160)=13.21, p_{FDR}=0.01	similar	n.s.

Network measure/AAL-area	Mean (SD) patients (n=114)	Mean (SD) healthy controls (n=54)	Difference between groups[a]	Difference between groups[b]	Difference between groups[c]
75. Left pallidum	0.47 (0.06)	0.47 (0.06)	F(1,160)=11.38, p_{FDR}=0.02	similar	similar
80. Right Heschl's gyrus	0.46 (0.07)	0.48 (0.06)	F(1,160)=14.32, p_{FDR}=0.01	similar	similar
81. Left superior temporal gyrus	0.42 (0.04)	0.45 (0.03)	F(1,160)=14.00, p_{FDR}=0.01	similar	n.s.
82. Right superior temporal gyrus	0.42 (0.04)	0.45 (0.03)	F(1,160)=12.94, p_{FDR}=0.01	similar	similar
84. Right temporal pole	In n=151 sample: 0.44 (0.03)	0.44 (0.03)	n.s.	F(1,143)=9.89, p_{FDR}=0.03	similar
85. Left middle temporal gyrus	0.42 (0.03)	0.44 (0.03)	F(1,160)=22.56, p_{FDR}=0.001	similar	similar
86. Right middle temporal gyrus	In n=151 sample: 0.42 (0.03)	0.45 (0.03)	n.s.	F(1,142)=7.77, p_{FDR}=0.04	n.s.
89. Left inferior temporal gyrus	In n=151 sample: 0.44 (0.04)	0.46 (0.05)	n.s.	F(1,143)=7.99, p_{FDR}=0.04	n.s.
Difference in normalized path length (λ)					
2. Right precentral gyrus	In n=151 sample: 1.04 (0.02)	1.05 (0.02)	n.s.	F(1,143)=7.83, p_{FDR}=0.04	n.s.
13. Left inferior frontal triangularis	1.06 (0.02)	1.07 (0.02)	F(1,154)=10.01, p_{FDR}=0.02	similar	n.s.
14. Right inferior frontal triangularis	In n=151 sample: 1.06 (0.02)	1.07 (0.02)	n.s.	F(1,142)=11.32, p_{FDR}=0.02	n.s.
26. Right medial orbital superior frontal gyrus	In n=151 sample: 1.07 (0.02)	1.08 (0.02)	n.s.	F(1,142)=7.80, p_{FDR}=0.04	
46. Right cuneus	1.04 (0.02)	1.06 (0.03)	F(1,160)=11.74, p_{FDR}=0.01	similar	n.s.
57. Left postcentral gyrus	In n=151 sample: 1.05 (0.02)	1.06 (0.03)	n.s.	F(1,143)=7.84, p_{FDR}=0.04	n.s.
58. Right postcentral gyrus	In n=151 sample: 1.04 (0.02)	1.06 (0.03)	n.s.	F(1,142)=8.76, p_{FDR}=0.04	n.s.
69. Left paracentral lobule	1.03 (0.02)	1.05 (0.02)	F(1,160)=9.82, p_{FDR}=0.03	similar	similar
77. Left thalamus	In n=151 sample: 1.07 (0.02)	1.08 (0.02)	n.s.	F(1,143)=8.34, p_{FDR}=0.04	n.s.
81. Left superior temporal gyrus	In n=151 sample: 1.07 (0.02)	1.07 (0.01)	n.s.	F(1,143)=9.03, p_{FDR}=0.03	n.s.
Difference in normalized clustering coefficient (γ)					

Network measure/AAL-area	Mean (SD) patients (n=114)	Mean (SD) healthy controls (n=54)	Difference between groups[a]	Difference between groups[b]	Difference between groups[c]
1. Left precentral gyrus	In n=151 sample: 1.55 (0.14)	1.63 (0.1)	n.s.	F(1,143)=8.58, p_{FDR}=0.04	F(1,109)=11.59, p_{FDR}=0.03
2. Right precentral gyrus	In n=151 sample: 1.56 (0.13)	1.64 (0.11)	n.s.	F(1,143)=9.09, p_{FDR}=0.03	n.s.
8. Right middle frontal gyrus	In n=151 sample: 1.54 (0.14)	1.62 (0.11)	n.s.	F(1,142)=7.71, p_{FDR}=0.045	n.s.
14. Right inferior frontal triangularis	In n=151 sample: 1.58 (0.15)	1.66 (0.11)	n.s.	F(1,142)=10.42, p_{FDR}=0.02	n.s.
27. Left gyrus rectus	In n=151 sample: 1.55 (0.28)	1.74 (0.28)	n.s.	F(1,140)=7.61, p_{FDR}=0.045	F(1,106)=11.65, p_{FDR}=0.03
35. Left posterior cingulate gyrus	In n=151 sample: 1.72 (0.23)	1.83 (0.19)	n.s.	F(1,143)=7.79, p_{FDR}=0.04	n.s.
44. Right calcarine sulcus	In n=151 sample: 1.40 (0.19)	1.52 (0.16)	n.s.	F(1,143)=11.41, p=0.002, p_{FDR}=0.02	n.s.
45. Left cuneus	In n=151 sample: 1.32 (0.14)	1.40 (0.13)	n.s.	F(1,143)=8.30, p_{FDR}=0.04	n.s.
51. Left middle occipital gyrus	In n=151 sample: 1.53 (0.16)	1.59 (0.14)	n.s.	F(1,143)=7.70, p_{FDR}=0.045	n.s.
52. Right middle occipital gyrus	In n=151 sample: 1.53 (0.15)	1.61 (0.14)	n.s.	F(1,143)=9.39, p_{FDR}=0.03	n.s.
57. Left postcentral gyrus	In n=151 sample: 1.47 (0.14)	1.54 (0.12)	n.s.	F(1,143)=9.33, p_{FDR}=0.03	F(1,109)=10.09, p_{FDR}=0.03
64. Right supramarginal gyrus	In n=151 sample: 1.47 (0.15)	1.54 (0.13)	n.s.	F(1,143)=7.35, p_{FDR}=0.049	n.s.
73. Left putamen	In n=151 sample: 1.59 (0.15)	1.66 (0.15)	n.s.	F(1,143)=7.53, p_{FDR}=0.046	n.s.
80. Right Heschl gyrus	In n=151 sample: 1.69 (0.29)	1.79 (0.24)	n.s.	F(1,143)=9.74, p_{FDR}=0.03	n.s.
85. Left middle temporal gyrus	In n=151 sample: 1.56 (0.15)	1.65 (0.13)	n.s.	F(1,143)=10.59, p_{FDR}=0.02	F(1,109)=11.03, p_{FDR}=0.03
Difference in small-world coefficient (σ)					

Network measure/AAL-area	Mean (SD) patients (n=114)	Mean (SD) healthy controls (n=54)	Difference between groups[a]	Difference between groups[b]	Difference between groups[c]
1. Left precentral gyrus	In n=151 sample: 1.49 (0.11)	1.55 (0.09)	n.s.	F(1,143)=8.27, p_{FDR}=0.04	F(1,109)=11.60, p_{FDR}=0.03
2. Right precentral gyrus	In n=151 sample: 1.50 (0.11)	1.56 (0.09)	n.s.	F(1,143)=8.40, p_{FDR}=0.04	n.s.
8. Right middle frontal gyrus	In n=151 sample: 1.46 (0.12)	1.52 (0.09)	n.s.	F(1,142)=7.39, p_{FDR}=0.049	n.s.
14. Right inferior frontal triangularis	In n=151 sample: 1.49 (0.13)	1.55 (0.1)	n.s.	F(1,142)=8.51, p_{FDR}=0.04	n.s.
27. Left gyrus rectus	In n=151 sample: 1.44 (0.25)	1.60 (0.23)	n.s.	F(1,140)=7.64, p_{FDR}=0.045	F(1,106)=12.76, p_{FDR}=0.03
44. Right calcarine sulcus	In n=151 sample: 1.31 (0.18)	1.42 (0.15)	n.s.	F(1,143)=11.57, p=0.003, p_{FDR}=0.02	n.s.
45. Left cuneus	In n=151 sample: 1.25 (0.12)	1.32 (0.11)	n.s.	F(1,143)=7.62, p_{FDR}=0.045	n.s.
51. Left middle occipital gyrus	In n=151 sample: 1.44 (0.14)	1.48 (0.13)	n.s.	F(1,143)=8.15, p_{FDR}=0.04	n.s.
52. Right middle occipital gyrus	In n=151 sample: 1.44 (0.14)	1.51 (0.13)	n.s.	F(1,143)=9.45, p_{FDR}=0.03	n.s.
80. Right Heschl gyrus	In n=151 sample: 1.60 (0.27)	1.68 (0.23)	n.s.	F(1,143)=7.95, p_{FDR}=0.04	n.s.
85. Left middle temporal gyrus	In n=151 sample: 1.45 (0.13)	1.53 (0.11)	n.s.	F(1,143)=10.52, p_{FDR}=0.02	F(1,109)=10.90, p_{FDR}=0.03

Corrected for education, total gray matter volume, local gray matter volume, age and sex. Only differences significant after FDR-correction for 540 tests are shown.

[a]N=114 patients and 54 healthy controls.

[b]Only including patients with schizophrenia (n=97) and healthy controls (n=54).

[c]Only including patients for which additional insight measures were available (n=62) and healthy controls (n=54).

Abbreviations: SD=standard deviation; AAL=automated anatomical labeling; n.s.=not significant; similar=similar as in whole sample.

Table S7. Associations between global gray matter network measures and insight (i.e. PANSS G12) with additional correction for age and sex.

	G12[a]	G12[b]	G12[c]
Path length (L)	r_s=-0.12, *p*=0.22	r_s=-0.14, *p*=0.19	r_s=-0.09, *p*=0.52
Clustering coefficient (CC)	r_s=-0.08, *p*=0.42	r_s=-0.09, *p*=0.38	r_s=-0.07, *p*=0.60
Betweenness centrality (BC)	r_s=0.09, *p*=0.36	r_s=0.10, *p*=0.35	**r_s=0.23, *p*=0.08, p_{FDR}=0.08**
Normalized path length (λ)	r_s=-0.15, *p*=0.11	**r_s=-0.18, *p*=0.09, p_{FDR}=0.09**	r_s=-0.15, *p*=0.26
Normalized clustering coefficient (γ)	r_s=-0.12, *p*=0.20	r_s=-0.11, *p*=0.30	r_s=-0.13, *p*=0.35
Small-world coefficient (σ)	r_s=-0.12, *p*=0.21	r_s=-0.10, *p*=0.33	r_s=-0.14, *p*=0.31

Corrected for total gray matter volume, age and sex.

[a]n=114 patients.

[b]n=97 patients, only including patients with schizophrenia.

[c]n=62 patients, only including patients with schizophrenia for whom additional insight measures were available.

NB: Higher insight is reflected by lower PANSS G12 scores.

Abbreviation: G12=item 12 of the General Psychopathology subscale of the Positive and Negative Syndrome Scale.

Table S8. Associations between global gray matter network measures and insight with additional correction for age and sex.

	SAIE AI	SAIE RS	SAIE NT	SAIE sub	BCIS SR	BCIS SC	BCIS ci
Path length (L)	r_s=0.17, *p*=0.21	r_s=-0.11, *p*=0.40	r_s=0.05, *p*=0.70	r_s=0.12, *p*=0.35	r_s=0.16, *p*=0.23	r_s=-0.14, *p*=0.28	r_s=0.21, *p*=0.11
Clustering coefficient (CC)	r_s=0.12, *p*=0.38	**r_s=0.31, *p*=0.02, p_{FDR}=0.08**	r_s=0.04, *p*=0.75	r_s=0.07, *p*=0.62	r_s=0.01, *p*=0.97	r_s=-0.03, *p*=0.81	r_s=0.01, *p*=0.97
Betweenness centrality (BC)	r_s=-0.18, *p*=0.18	**r_s=-0.32, *p*=0.02, p_{FDR}=0.08**	r_s=-0.02, *p*=0.89	r_s=-0.19, *p*=0.14	r_s=-0.10, *p*=0.45	r_s=0.04, *p*=0.76	r_s=-0.10, *p*=0.48
Normalized path length (λ)	**r_s=0.24, *p*=0.06, p_{FDR}=0.08**	r_s=-0.04, *p*=0.80	r_s=0.09, *p*=0.48	r_s=0.19, *p*=0.16	r_s=0.20, *p*=0.13	r_s=-0.15, *p*=0.27	**r_s=0.23, *p*=0.08, p_{FDR}=0.08**
Normalized clustering coefficient (γ)	r_s=0.19, *p*=0.14	r_s=0.06, *p*=0.65	r_s=0.16, *p*=0.24	r_s=0.14, *p*=0.30	r_s=0.21, *p*=0.12	r_s=-0.22, *p*=0.10	**r_s=0.25, *p*=0.06, p_{FDR}=0.08**
Small-world coefficient (σ)	r_s=0.18, *p*=0.16	r_s=0.06, *p*=0.65	r_s=0.19, *p*=0.14	r_s=0.13, *p*=0.31	r_s=0.21, *p*=0.11	**r_s=-0.24, *p*=0.06, p_{FDR}=0.08**	**r_s=0.26, *p*=0.05, p_{FDR}=0.08**

NB: n=62 patients. Corrected for total gray matter volume, age and sex. Correlations between SAIE RS and graph metrics are additionally corrected for PANSS positive symptom scores. Higher insight is reflected by higher SAI-E scores, higher BCIS self-reflectiveness (SR), and composite index (ci) scores and lower BCIS self-certainty (SC) scores.

Abbreviations: SAIE=Schedule for Assessment of Insight – Expanded; AI=Awareness of illness; RS=Relabeling of symptoms; NT=Need for treatment; sub=subtotal score; BCIS=Beck Cognitive Insight Scale; SR=self-reflectiveness; SC=self-certainty; ci=composite index score.

Table S9. Associations between local gray matter network measures and insight with additional correction for age and sex.

	G12	SAIE AI	SAIE RS	SAIE NT	SAIE sub	BCIS SR	BCIS SC	BCIS ci
Path length (L)								
1. Left precentral gyrus								0.42
2. Right precentral gyrus		0.37						0.39
4. Right superior frontal gyrus								0.43
8. Right middle frontal gyrus		0.37						
23. Left medial superior frontal gyrus						0.43		0.45
32. Right anterior cingulate gyrus		0.39						
34. Right middle cingulate gyrus								0.36
45. Left cuneus						0.38		
51. Left middle occipital gyrus						0.36		0.37
69. Left paracentral lobule						0.39		0.41
Clustering coefficient (CC)								
5. Left superior frontal orbitalis			0.39					
7. Left middle frontal gyrus			0.37					
12. Right inferior frontal opercularis			0.44					
39. Left parahippocampal gyrus			0.40					
56. Right fusiform gyrus			0.39					
58. Right postcentral gyrus			0.36					
61. Left inferior parietal lobule			0.36					
66. Right angular gyrus			0.41					
Betweenness centrality (BC)								
14. Right inferior frontal triangularis	0.38							
Normalized path length (λ)								
2. Right precentral gyrus		0.36						0.38
4. Right superior frontal gyrus						0.36		0.41
8. Right middle frontal gyrus		0.42						
23. Left medial superior frontal gyrus						0.37		0.42
32. Left anterior cingulate gyrus	-0.36	0.39	0.36					
69. Left paracentral lobule						0.36		
78. Right thalamus		0.37						0.37
81. Left superior temporal gyrus						0.39		
Normalized clustering coefficient (γ)								
6. Right superior frontal orbitalis						0.36		
9. Left middle frontal orbitalis						0.36		
53. Left inferior occipital gyrus						0.35		0.36
58. Right postcentral gyrus						0.36		
Small-world coefficient (σ)								
6. Right superior frontal orbitalis						0.37		
7. Left middle frontal gyrus								0.36
9. Left middle frontal gyrus orbitalis						0.37		
16. Right inferior frontal gyrus orbitalis								0.36
53. Left inferior occipital gyrus						0.38		0.39

NB: n=62 patients. Corrected for total and local gray matter volume, and age and sex. Correlations between SAIE RS and graph metrics are additionally corrected for PANSS positive symptom scores. Higher insight is reflected by lower PANSS G12 scores, higher SAI-E scores, higher BCIS self-reflectiveness (SR), and composite index (ci) scores and lower BCIS self-certainty (SC) scores. Spearman correlations are shown for correlations significant at trend-level ($0.05 \geq p > 0.1$) after FDR-correction for 720 tests, no correlations were significant at $p<0.05$ after FDR-correction for 720 tests.

Abbreviations: G12= item 12 of the General Psychopathology subscale of the Positive and Negative Syndrome Scale; SAIE=Schedule for Assessment of Insight – Expanded; AI=Awareness of illness; RS=Relabeling of symptoms; NT=Need for treatment; sub=subtotal score; BCIS=Beck Cognitive Insight Scale; SR=self-reflectiveness; SC=self-certainty; ci=composite index score.

Figures

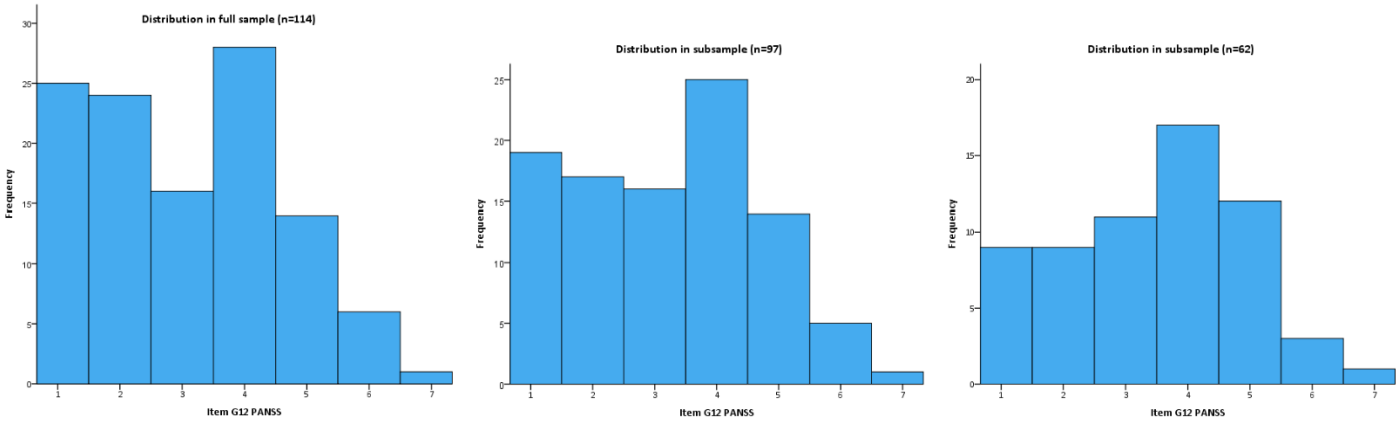

Figure S1. Distribution of scores on item 12 of the general psychopathology subscale (G12) of the Positive and Negative Syndrome Scale (PANSS).

NB: full sample (n=114) includes all patients, while subsamples include only patients with schizophrenia (n=97) or only patients with schizophrenia for whom additional insight measures were available (n=62).

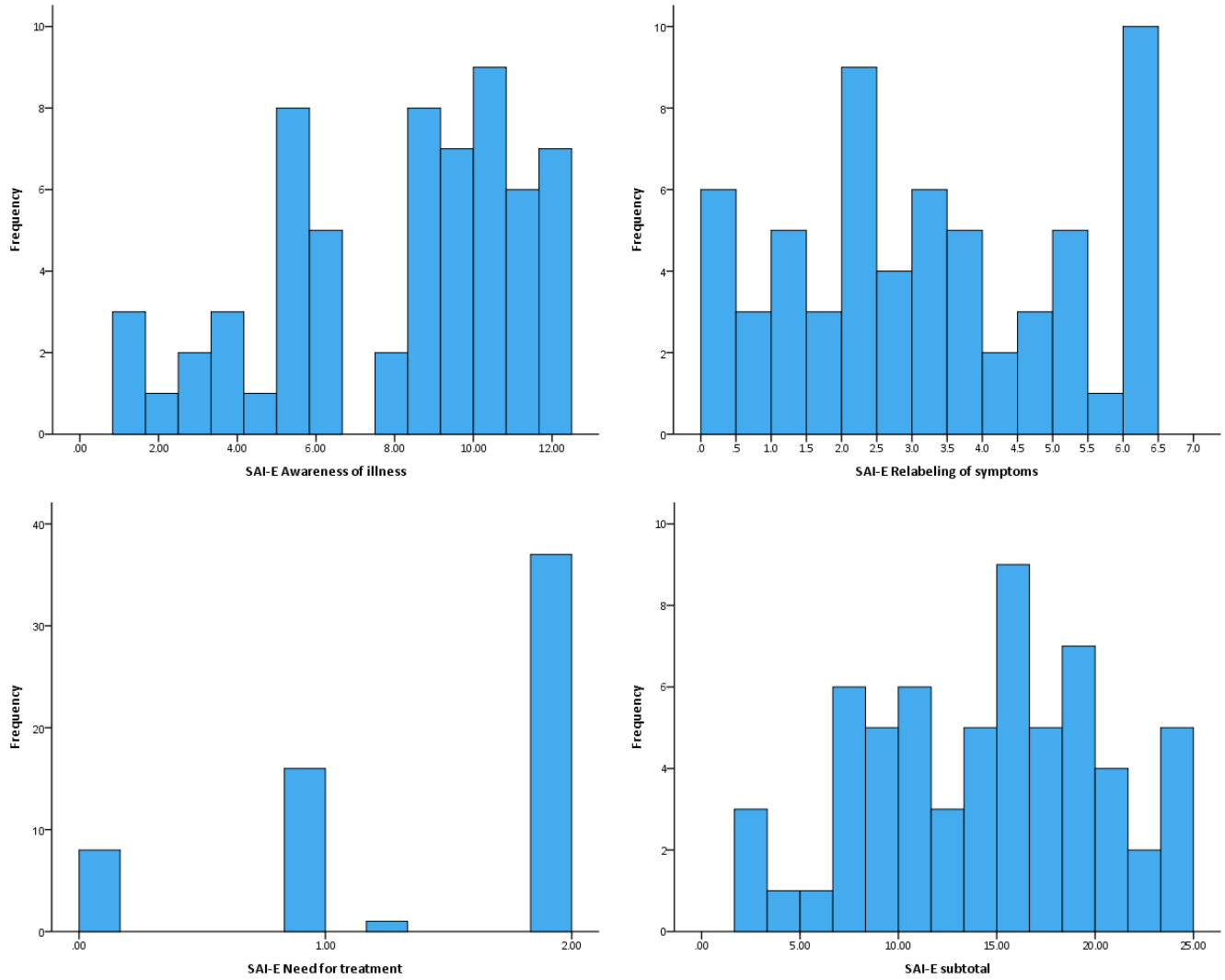

Figure S2. Distribution of scores on the Schedule for the Assessment of Insight – Expanded in subsample for whom this measure was available (n=62).

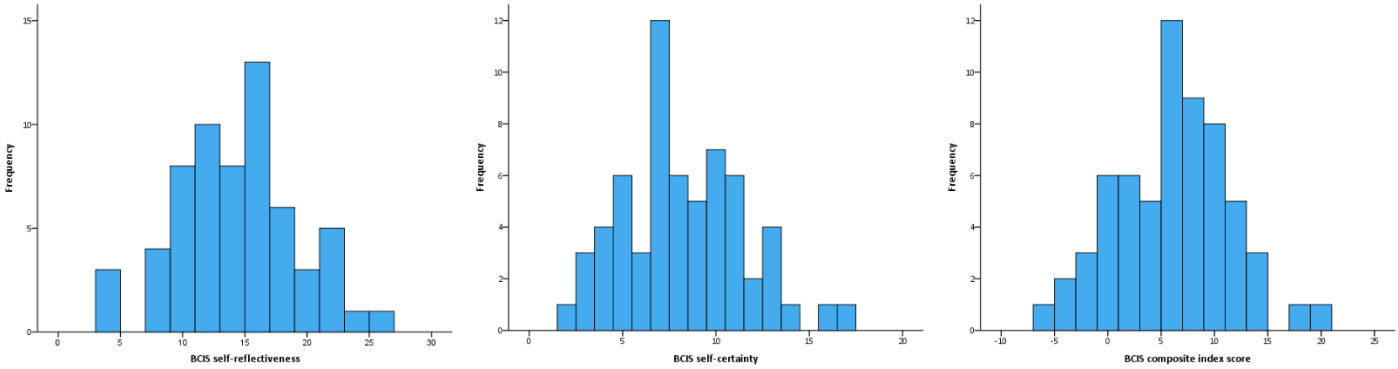

Figure S3. Distribution of scores on the Beck Cognitive Insight Scale (BCIS) in subsample for whom this measure was available (n=62).

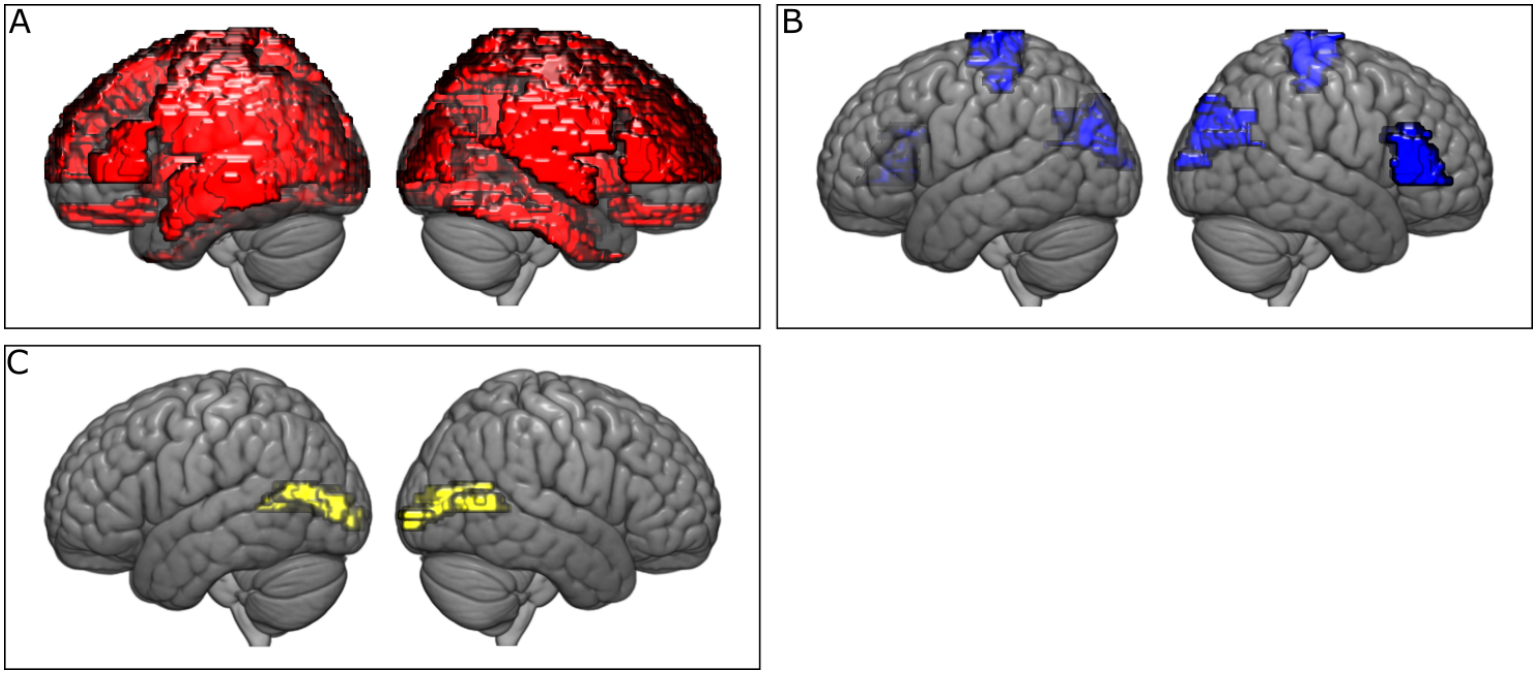

Figure S4. Plots of the AAL-areas that showed lower clustering coefficient (A), lower normalized path length (B), and lower normalized clustering coefficient and small-world coefficient (C) in patients compared to healthy controls. Lateral areas are displayed with opaque coloring, medial areas with transparent coloring. This figure was created with WFU PickAtlas (Tzourio-Mazoyer *et al.* 2002; Maldjian J.A. *et al.* 2003; Maldjian *et al.* 2004) and MRIcroGL (Rorden & Brett 2000).

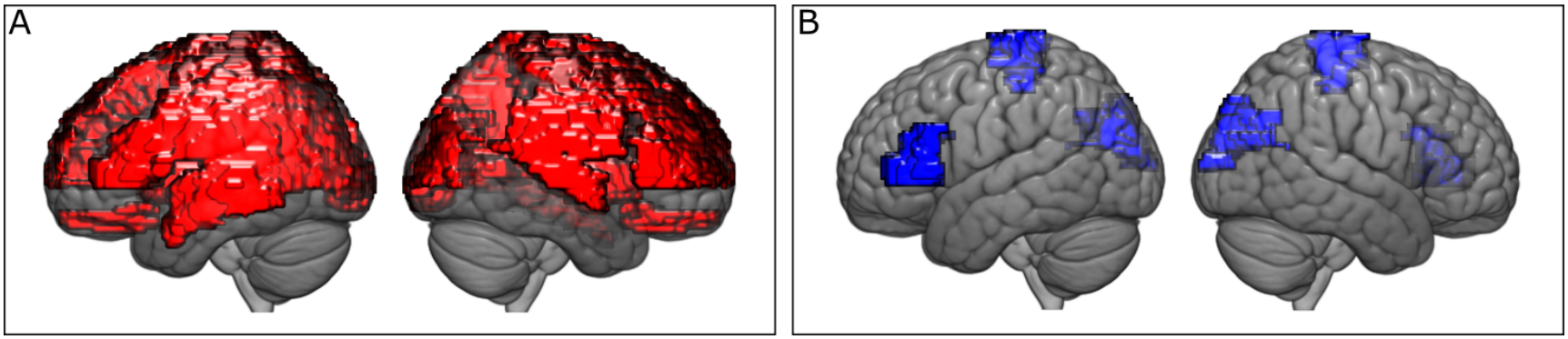

Figure S5. Plots of the AAL-areas that showed lower clustering coefficient (A) and lower normalized path length (B) in patients compared to healthy controls after additional correction for age and sex. Lateral areas are displayed with opaque coloring, medial areas with transparent coloring. This figure was created with WFU PickAtlas (Tzourio-Mazoyer *et al.* 2002; Maldjian J.A. *et al.* 2003; Maldjian *et al.* 2004) and MRIcroGL (Rorden & Brett 2000).

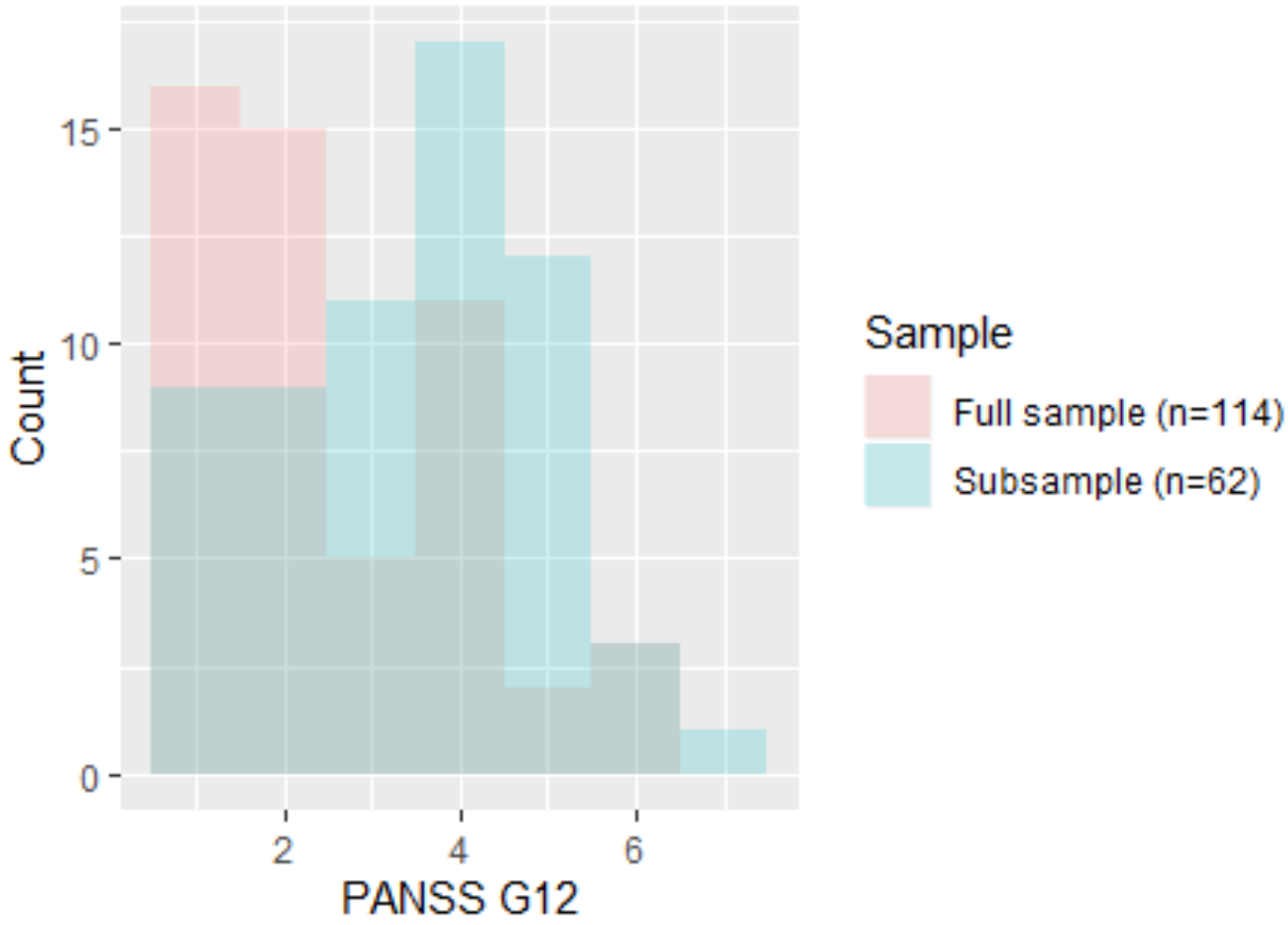

Figure S6. Overlay of distributions of scores on item G12 of the general psychopathology subscale (G12) of the Positive and Negative Syndrome Scale (PANSS) in the full sample (n=114) and subsample (n=62).

References

Bassett DS, Bullmore E, Verchinski BA, Mattay VS, Weinberger DR, Meyer-Lindenberg A (2008). Hierarchical organization of human cortical networks in health and schizophrenia. *Journal of Neuroscience* **28**, 9239–9248.

Birchwood M, Smith J, Drury V, Healy J, Macmillan F, Slade M (1994). A self-report Insight Scale for psychosis: reliability, validity and sensitivity to change. *Acta Psychiatrica Scandinavica* **89**, 62–67.

Dlabac-de Lange JJ, Bais L, van Es FD, Visser BGJ, Reinink E, Bakker B, van den Heuvel ER, Aleman A, Knegtering H (2015). Efficacy of bilateral repetitive transcranial magnetic stimulation for negative symptoms of schizophrenia: results of a multicenter double-blind randomized controlled trial. *Psychological Medicine* **45**, 1263–1275.

Humphries MD, Gurney K (2008). Network 'small-world-ness': A quantitative method for determining canonical network equivalence. *PLoS ONE* **3**

Kay SR, Fiszbein A, Opler LA (1987). The positive and negative syndrome scale (PANSS) for schizophrenia. *Schizophrenia Bulletin* **13**, 261–276.

Liemburg EJ, van Es F, Knegtering H, Aleman A (2017). Effects of aripiprazole versus risperidone on brain activation during planning and social-emotional evaluation in schizophrenia: A single-blind randomized exploratory study. *Progress in Neuro-Psychopharmacology and Biological Psychiatry* **79**, 112–119.

Maldjian J.A., Laurienti P.J., Kraft R.A., Burdette J.H. (2003). An automated method for neuroanatomic and cytoarchitectonic atlas-based interrogation of fMRI data sets. *NeuroImage* **19**, 1233–1239.

Maldjian JA, Laurienti PJ, Burdette JH (2004). Precentral gyrus discrepancy in electronic versions of the Talairach atlas. *NeuroImage* **21**, 450–455.

Van der Meer L, Swart M, Van Der Velde J, Pijnenborg GHM, Wiersma D, Bruggeman R, Aleman A (2014). Neural correlates of emotion regulation in patients with schizophrenia and non-affected siblings.

PLoS ONE **9**

Palaniyappan L, Hodgson O, Balain V, Iwabuchi S, Gowland P, Liddle P (2019). Structural covariance and cortical reorganisation in schizophrenia: a MRI-based morphometric study. *Psychological Medicine* **49**, 412–420.

Pijnenborg GHM, Van der Gaag M, Bockting CLH, Van der Meer L, Aleman A (2011). REFLEX, a social-cognitive group treatment to improve insight in schizophrenia: study protocol of a multi-center RCT. *BMC Psychiatry* **11**, 161.

Rorden C, Brett M (2000). Stereotaxic display of brain lesions. *Behavioural Neurology* **12**, 191–200.

Rubinov M, Sporns O (2010). Complex network measures of brain connectivity: Uses and interpretations. *NeuroImage* **52**, 1059–1069.

Tijms BM, Möller C, Vrenken H, Wink AM, de Haan W, van der Flier WM, Stam CJ, Scheltens P, Barkhof F (2013). Single-Subject Grey Matter Graphs in Alzheimer's Disease. *PLoS ONE* **8**, 1–9.

Tijms BM, Sprooten E, Job D, Johnstone EC, Owens DGC, Willshaw D, Series P (2015). Grey matter networks in people at increased familial risk for schizophrenia. *Schizophrenia Research* **168**, 1–8.

Tzourio-Mazoyer N, Landeau B, Papathanassiou D, Crivello F, Etard O, Delcroix N, Mazoyer B, Joliot M (2002). Automated anatomical labeling of activations in SPM using a macroscopic anatomical parcellation of the MNI MRI single-subject brain. *NeuroImage* **15**, 273–289.

van der Velde J, van Tol M-J, Goerlich-Dobre KS, Gromann PM, Swart M, de Haan L, Wiersma D, Bruggeman R, Krabbendam L, Aleman A (2014). Dissociable morphometric profiles of the affective and cognitive dimensions of alexithymia. *Cortex* **54**, 190–199.

Watts DJ, Strogatz SH (1998). Collective dynamics of small-world networks. *Nature* **393**, 440–442.

van Wijk BCM, Stam CJ, Daffertshofer A (2010). Comparing brain networks of different size and connectivity density using graph theory. *PLoS ONE* **5**